Commun Nonlinear Sci Numer Simulat 44 (2017) 120–129

Contents lists available at ScienceDirect

Commun Nonlinear Sci Numer Simulat

journal homepage: www.elsevier.com/locate/cnsns

Research paper

Rogue waves of a $(3+1)$-dimensional nonlinear evolution equation

Yu-bin Shi*, Yi Zhang

Department of Mathematics, Zhejiang Normal University, Jinhua 321004, P R China

ARTICLE INFO

Article history:
Received 2 May 2016
Accepted 22 July 2016
Available online 6 August 2016

Keywords:
$(3+1)$-dimensional nonlinear evolution equation
Rogue waves
Hirota bilinear method

ABSTRACT

General high-order rogue waves of a $(3+1)$-dimensional Nonlinear Evolution Equation ((3+1)-d NEE) are obtained by the Hirota bilinear method, which are given in terms of determinants, whose matrix elements possess plain algebraic expressions. It is shown that the simplest (fundamental) rogue waves are line rogue waves which arise from the constant background with a line profile and then disappear into the constant background again. Two subclass of nonfundamental rogue waves are analyzed in details. By proper means of the regulations of free parameters, the dynamics of multi-rogue waves and high-order rogue waves have been illustrated in (x,t) plane and (y,z) plane by three dimensional figures.

1. Introduction

The phenomena of rogue waves [1], mostly known as large and spontaneous ocean surface waves, should be responsible for a large number of maritime disasters. In the past decades, the experimental observation and theoretical analysis on rogue waves have ranged from Bose-Einstein condensates [2,3] to optical system [4–6], ocean [7], superfluids [8], plasma [9,10] and so on [11]. Mathematically, the fundamental rogue wave solution (i.e., first-order rogue wave solution) was firstly obtained in the nonlinear schrödinger (NLS) equation by Peregrine [12], which is located in both space and time, and the rogue wave solution also can be called Peregrine solution. Recently, the higher-order rogue wave solutions in NLS equation were studied in many articles [13–19]. It is seen that the higher-order rogue waves can be treat as superpositions of several fundamental rogue waves, and the superpositions can create higher amplitudes which still keep located both of space and time. What's more, the hierarchy of rogue wave solutions for other soliton equations have also been reported in references [20–29].

In addition to the one dimensional rogue wave studied so far, rogue waves in two dimensional have also derived a lot of attention. Furthermore, the two-dimensional analogue of rogue wave, expressed by more complicated rational form, has been recently reported in the Davey - Stewartson (DS) systems [30,31], Kadomtsev-Petviashvili-I equation [32,33], Yajima-Oikawa system [34], and the Fokas system [28] and so on [35,36]. As the $(3+1)$-dimensional systems also play an important role in physical systems, a natural motivation is to investigate rogue waves in $(3+1)$-dimensional model equations. Recently, Zha have derived the fundamental rogue wave in a $(3+1)$-dimensional Nonlinear Evolution Equation by a simple symbolic computation approach [37].

* Corresponding author.
E-mail address: 617437638@qq.com, 15268637019@163.com (Y.-b. Shi).

http://dx.doi.org/10.1016/j.cnsns.2016.07.021
1007-5704/

In this Letter, we consider a $(3+1)$-dimensional Nonlinear Evolution Equation ($(3+1)$-d NEE)

$$3w_{xz} - (2w_t + w_{xxx} - 2ww_x)_y + 2(w_x\,\partial_x^{-1}w_y)_x = 0\,, \tag{1}$$

is a new integrable equation, was first introduced in the study of the algebraic geometrical solutions [38]. Although the application of this $(3+1)$-dimensional mode for physics or other science is not clear, but it is not hard to find that the relationship of the (3+1)-dimensional NEE (1) and the famous Kortewege de Vries (KdV) equation is very strong. The KdV equation is given by

$$u_{t'} - 6u\,u_{x'} + u_{x'x'x'} = 0\,. \tag{2}$$

Under the construction $u(x',t') \to w(x,t)\,, x' \to \frac{1}{\sqrt{3}}x\,, t' \to \frac{1}{6\sqrt{3}}t$, the KdV equation can be transformed into the main term $2w_t + w_{xxx} - 2ww_x$ possessed by the (3+1)-d NEE (1). Recently, various nonlinear types of KdV equations such as Kadomtsev - Petviashvili equation have been developed in a large range of physical phenomena. As an extension of the KdV equation, the (3+1)-d NEE (1) may be applied to model shallow water waves and short waves in nonlinear dispersive models. Except for the fundamental rogue waves obtained by Zha [37], the other solutions including solitons [39–42], positions [42] have been derived by Hirota bilinear method, Darboux transformation or some other method. So investigating the other kinds of rogue waves and the general high-order rouge waves of the $(3+1)$-d NEE is an important motivation.

In our present work, we obtain the general high-order rogue waves of the $(3+1)$-d NEE (1), which are expressed in term of determinants based on the Hirota's bilinear method [43] and KP hierarchy reduction method [44]. The basic idea is to treat $(3+1)$-d NEE as a constrained KP hierarchy. Then, we derive the rational solutions of the $(3+1)$-d NEE from the rational solutions of KP hierarchy. What's more, the rational solutions can be in a simple representation. Furthermore,we could investigate the dynamic behaviors of high dimensional rogue waves of the $(3+1)$-d NEE.

The outline of the paper is organized as follows. In Section 2, the bilinear forms and rational solutions of the $(3+1)$-d NEE will be given. In Section 3, the form of rogue waves for the $(3+1)$-d NEE is studied in details, and typical dynamics of the obtained rogue waves is analyzed and illustrated. The Section 4 contains a summary and discussion.

2. The rational solutions of (3+1)-d NEE equation

In this section, we focus on the rational solutions of the $(3+1)$-d NEE (1). Firstly, through the dependent variable transformation

$$w = -(2\log\, f)_{xx}, \tag{3}$$

the (3+1)-d NEE Eq. (1) can be transformed into the bilinear forms

$$(3D_xD_z - 2D_yD_t - D_yD_x^3)f\cdot f = 0. \tag{4}$$

Here f is a real function with respect to variables x, y, z and t, and the operator D is the Hirota's bilinear differential operator [43] defined by $P(D_x, D_y, D_t,)F(x,y,t\cdots)\cdot G(x,y,t,\cdots) = P(\partial_x - \partial_{x'}, \partial_y - \partial_{y'}, \partial_t - \partial_{t'}, \cdots)F(x,y,t,\cdots)G(x',y',t',\cdots)|_{x'=x,y'=y,t'=t}$, where P is a polynomial of D_x, D_y, D_t, $\cdots$.

Theorem 1. *The (3+1)-d NEE Eq. (1) has rational solutions*

$$u = -2(\log f)_{xx}, \tag{5}$$

where

$$f = \det_{1\le i,j\le N}(m_{i,j}), \tag{6}$$

and the matrix elements in f are defined by

$$m_{i,j} = \left(\sum_{k=0}^{n_i} c_{ik}(p_i\partial_{p_i} + \xi_i')^{n_i-k} \times \sum_{l=0}^{n_j} c_{jl}^*(p_j^*\partial_{p_j^*} + \xi_j'^*)^{n_j-l}\right)\frac{1}{p_i + p_j^*}, \tag{7}$$

with

$$\xi_i' = p_i\,x + 2\,i\,p_i^2\,y + 3\,p_i^3\,t + 4\,i\,p_i^4\,z. \tag{8}$$

Here asterisk denotes complex conjugation, and i, j, n_i, n_j are arbitrary positive integers, p_i and p_j are arbitrary complex constants.

By a scaling of $m_{ij}^{(n)}$, we can normalize $a_0 = 1$ without loss of generality, and thus hereafter set $a_0 = 1$. These rational solutions can also be expressed in terms of Schur polynomials as shown in [19,30]. What's more, the non-singularity of these rational solutions have been proof in [19,35] if the real parts of wave numbers p_i $(1 \le i \le N)$ are all positive or negative. Next, we will provide the proof of this theorem.

Lemma 1. *Let $m_{ij}^{(n)}$ $\psi_i^{(n)}$ and $\phi_j^{(n)}$ be functions of variables x_{-1}, x_1 and x_2 satisfying the following differential and difference relations,*

$$\begin{aligned}
\partial_{x_1} m_{ij}^{(n)} &= \psi_i^{(n)}\phi_j^{(n)},\\
\partial_{x_2} m_{ij}^{(n)} &= \psi_i^{(n+1)}\phi_j^{(n)} + \psi_i^{(n)}\phi_j^{(n-1)},\\
\partial_{x_3} m_{ij}^{(n)} &= \psi_i^{(n+2)}\phi_j^{(n)} + \psi_i^{(n+1)}\phi_j^{(n-1)} + \psi_i^{(n)}\phi_j^{(n-2)},\\
\partial_{x_4} m_{ij}^{(n)} &= \psi_i^{(n+3)}\phi_j^{(n)} + \psi_i^{(n+2)}\phi_j^{(n-1)} + \psi_i^{(n+1)}\phi_j^{(n-2)} + \psi_i^{(n)}\phi_j^{(n-3)},\\
m_{ij}^{(n+1)} &= m_{ij}^{(n)} + \psi_i^{(n)}\phi_j^{(n+1)},\\
\partial_{x_v}\psi_i &= \psi_i^{(n+v)},\\
\partial_{x_v}\phi_j &= -\phi_j^{(n-v)} \quad (v = 1, 2, 3, 4).
\end{aligned} \tag{9}$$

then the determinant

$$\tau_n = \det_{1\le i,j\le N}(m_{ij}^{(n)}) \tag{10}$$

satisfies the following bilinear equations

$$((D_{x_1}^3 + 2D_{x_3})D_{x_2} - 3D_{x_1}D_{x_4})\tau_n\cdot\tau_n = 0, \tag{11}$$

This Lemma can been proved by a similar way as the proof of the Lemma 1 of Ref. [30,36], thus we omit the proof of this Lemma in this paper. Next we use this Lemma to proof Theorem 1.

Proof of Theorem 1. In order to prove Theorem 1, the following selection of functions $m_{ij}^{(n)}$, $\psi_i^{(n)}$ and $\phi_j^{(n)}$ is best to obtain rational solutions

$$\begin{aligned}
\psi_i^{(n)} &= A_i p_i^n e^{\xi_i},\\
\phi_j^{(n)} &= B_j(-q_j)^{-n}e^{\eta_j},\\
m_{ij}^{(n)} &= A_i B_j \frac{1}{p_i+q_j}\left(-\frac{p_i}{q_j}\right)^n e^{\xi_i+\eta_j},
\end{aligned}$$

where

$$\begin{aligned}
A_i &= \sum_{k=0}^{n_i} c_{ik}(p_i\partial_{p_i})^{n_i-k}, \qquad B_j = \sum_{l=0}^{n_j} d_{jl}\left(q_j\partial_{q_j}\right)^{n_j-l},\\
\xi_i &= p_i x_1 + p_i^2 x_2 + p_i^3 x_3 + p_i^4 x_4, \qquad \eta_j = q_i x_1 - q_i^2 x_2 + q_i^3 x_3 - q_i^4 x_4,
\end{aligned}$$

and for simplicity, the functions $m_{ij}^{(n)}$ can be rewritten as

$$m_{i,j}^{(n)} = e^{\xi_i+\eta_j}\left(-\frac{p_i}{q_j}\right)^n \sum_{k=0}^{n_i} c_{ik}(p_i\partial_{p_j} + \xi' + n)^{n_i-k} \sum_{l=0}^{n_j} d_{jl}(q_j\partial_{q_j} + \eta' - n)^{n_j-l}\frac{1}{p_i+q_j}, \tag{12}$$

where

$$\xi_i' = p_i x_1 + 2p_i^2 x_2 + 3p_i x_3 + 4p_i^4 x_4, \quad \eta_j' = q_j x_1 - 2q_j^2 x_2 + 3q_j^3 x_3 - 4q_j x_4.$$

here p_i, qj, c_{ik}, d_{jl} are arbitrary complex constants, and i, j, n_i, N are arbitrary positive integers.

Further, taking parameter constraints

$$q_j = p_j^*, \qquad d_{jl} = c_{jl}^* \tag{13}$$

and assuming x_1, x_3 are real, x_2, x_4 are pure imaginary, we have

$$\eta_j' = \xi_j'^*, \quad m_{ij}^*(n) = m_{ji}(-n), \quad \tau_n^* = \tau_{-n}. \tag{14}$$

Applying the change of independent variables $x_1 = x, x_2 = iy, x_3 = t, x_4 = iz$, and setting $\tau_0 = f$, the bilinear equation Eq. (11) can be transformed into the bilinear Eq. (4). Under the gauge transformation (3), the rational solutions of (3+1)-d NEE (1) given in Theorem 1 can be obtained form the rational solutions of Eq. (11). Thus the Theorem 1 have been proved. □

3. Dynamics of rogue waves in the (3+1)-d NEE

In this section, we are in a position to analyze the features and asymptotic behaviors of rogue waves in $(3+1)$-d NEE (1) equation in details. Firstly, we obtain the fundamental rogue waves (i.e., first-order rogue waves) from the Theorem 1.

3.1. Fundamental rogue waves in the (3+1)-d NEE

Setting $N=1\,, n_i=1$ in Theorem 1, the first-order rational solutions of the (3+1)-d NEE (1) can been given as the following form

$$w=-(2\log f)_{xx}, \tag{15}$$

with

$$\begin{aligned} f&=\left(\sum_{k=0}^{1}c_{1k}(p_1\partial_{p_1}+\xi_1^{'})^{1-k}\sum_{l=0}^{1}c_{1l}^{*}(p_1^{*}\partial_{p_1^{*}}+\xi_1^{'*})^{1-l}\right)\frac{1}{p_1+p_1^{*}},\\ &=\left(p_1\partial_{p_1}+\xi_1^{'}+c_{11}\right)\left(p_1^{*}\partial_{p_1^{*}}+\xi_1^{'*}+c_{11}^{*}\right)\frac{1}{p_1+p_1^{*}},\\ &=\frac{1}{p_1+p_1^{*}}\left[\left(\xi_1^{'}-\frac{p_1}{p_1+p_1^{*}}+c_{11}\right)\left(\xi_1^{'*}-\frac{p_1^{*}}{p_1+p_1^{*}}+c_{11}^{*}\right)+\frac{p_1p_1^{*}}{(p_1+p_1^{*})^2}\right], \end{aligned} \tag{16}$$

where

$$\xi_1^{'}=p_1x+2ip_1^2y+3p_1^3t+4ip_1^4z, \tag{17}$$

p_1 and c_{11} are arbitrary complex parameters. Actually, c_{11} can be eliminated after a shift of space and time coordinates, thus we can set $c_{11}=0$ without loss of generality. We assume $p_1=p_{1R}+ip_{1I}$ and then rewrite the above solutions as

$$f=\frac{1}{2p_{1R}}(\theta\,\theta^{*}+\theta_0), \tag{18}$$

where $\theta=l_1+il_2\,, l_1=p_{1R}x-4p_{1R}p_{1I}y+3p_{1R}(p_{1R}^2-3p_{1I}^2)t+16p_{1R}p_{1I}(p_{1I}^2-p_{1R}^2)z$ and $l_2=p_{1I}x+2(p_{1R}^2-p_{1I}^2)y+3p_{1I}(3p_{1R}^2-p_{1I}^2)t+4(p_{1R}^2-p_{1I}^2-2p_{1I}p_{1R})(p_{1R}^2-p_{1I}^2+2p_{1I}p_{1R})z$. Then, the final expression of the rational solutions is

$$w=4\frac{(p_{1R}^2+p_{1I}^2)(2l_1l_2-\theta_0)+(p_{1R}^2-p_{1I}^2)(l_1^2+l_2^2)}{(l_1^2+l_2^2+\theta_0)^2}, \tag{19}$$

As most $(2+1)$-dimensional systems studied before [28,30,31,34], there are also two different dynamics behaviors. When $p_{1R}\neq 0$, It can see that the rational solutions w (19) are constants along the trajectory $p_{1R}x-4p_{1R}p_{1I}y+3p_{1R}(p_{1R}^2-3p_{1I}^2)t+16p_{1R}p_{1I}(p_{1I}^2-p_{1R}^2)z=0$ and $p_{1I}x+2(p_{1R}^2-p_{1I}^2)y+3p_{1I}(3p_{1R}^2-p_{1I}^2)t+4(p_{1R}^2-p_{1I}^2-2p_{1I}p_{1R})(p_{1R}^2-p_{1I}^2+2p_{1I}p_{1R})z$. Whatever, at any given time, $t\to 0$ when (x, y, z) turns to infinity. Thus rational solutions w (19) are permanent lumps moving on the constant background when p_1 is complex. When $p_{1I}=0$ (i.e., p_1 is real), as $t\to\pm\infty$, the solutions describe line waves go to uniform constant background, and arise to much higher amplitude. Thus they are line rogue waves which 'appear from no where and disappear without a trace'. As we only focus on the rogue waves in the $(3+1)$-d NEE (1), we set p_i real parameters in the next part of this paper.

The solutions for parameter choice $c_{11}=0\,, p_1=1$ are shown in Fig. 1, which demonstrate the dynamics of the corresponding solution in six plane. It is seen that the first-order rational solutions behave quiet similar in (x, y) plane, (x, z) plane, (y, t) plane, (z, t) plane, so we just show the dynamics of the rational solution of the (3+1)-d NEE (1) in (x, y) plane as a representation of those four panels in this paper. Furthermore, the corresponding solutions in (x, y) plane or (y, z) plane behave as decaying line waves, next we demonstrate the different characters in detail.

For (x, t) plane and (y, z) plane, the rational solutions are decaying line waves, which are distinctly different from the moving line solitons. Firstly, for simplicity, we set $z=0$, and show the dynamics of the corresponding solutions w (19) in (x, t) plane with different parameters y. As shown in Fig. 2, when $y\to\pm\infty$, the solution uniformly approaches the constant background 0 everywhere in the (x, t) plane. But in appropriate y, the amplitudes of the line waves approach much bigger (see the $y=0$ panel in Fig. 2), which means the line waves are located at y. But the biggest amplitudes of the line waves is upside down, so we call this decaying line waves are dark line rogue waves, which have been illustrated in Ref. [19]. What is more interesting, the decaying line waves behave quiet complicated and funny in (z, y) plane. Setting $x=0$, it is seen in Fig. 3, as $t\to\pm\infty$, the line waves also do approach the constant background 0 in the (z, y) plane. But in a intermediate times, they approach their bigger amplitudes, and the maximum peak is upward(see the $t=-1$ panel in Fig. 3), which means this line waves behave as bright rogue waves. But soon afterwards, the maximum peak become downward, so the state of the line rogue waves changes and becomes dark rogue waves(see the $t=-\frac{1}{2}\,, 0\,, \frac{1}{2}$ panel in Fig. 3). What's more, after staying in dark rogue waves in a short period, the state of the line waves changes again. It is seen that the maximum peaks become upward again(see the $t=1, 2$ panel in Fig. 3), so the line waves become bright line rogue waves again. Finally,

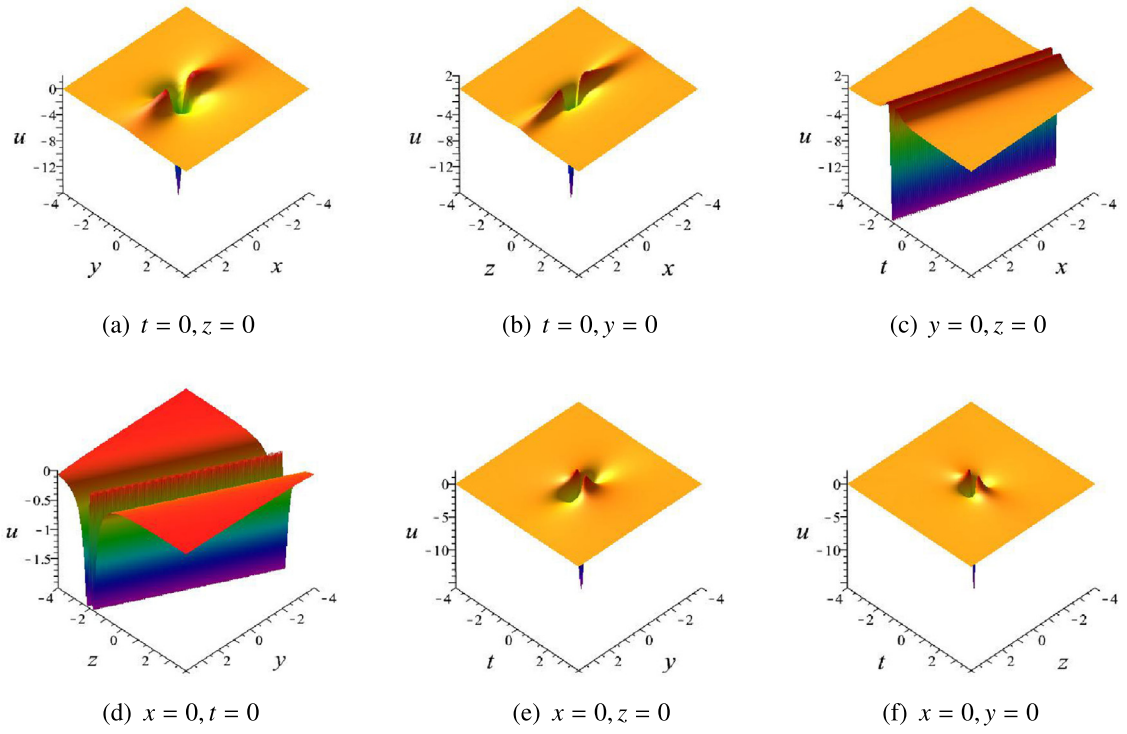

Fig. 1. (Color online) A fundamental rogue wave w (19) in $(3+1)$-NEE (1) with parameters $c_{11} = 0, c_{10} = 1, p_1 = 1$ in different panels (For interpretation of the references to colour in this figure legend, the reader is referred to the web version of this article).

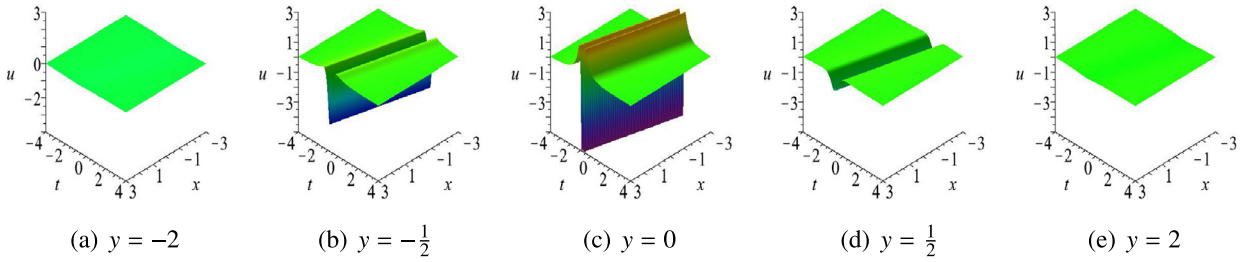

Fig. 2. (Color online) Dynamics of a fundamental rogue wave w (19) in $(3+1)$-NEE (1) with parameters $c_{11} = 0, c_{10} = 1, p_1 = 1, z = 0$ in (x, t) panel (For interpretation of the references to colour in this figure legend, the reader is referred to the web version of this article).

the line waves approach back to the constant background gain as $t \to +\infty$(see the $t = 5$ panel in Fig. 3). This kind of rogue waves, as to the author's best knowledge, have never been shown before, we call it bright-dark-bright rogue waves.

The above discussion just focus on $(3+1)$-dimensional fundamental rogue waves in the $(3+1)$-d NEE (1). Next we derive nonfundamental rogue waves from Theorem 1 by taking $N > 1$, or $n_i > 1$, or both. We consider two subclass of nonfundamental rogue waves (i.e., mutli-rogue waves and high-order rogue waves) in the coming part of this paper.

3.2. Multi-rogue waves in $(3+1)$-d NEE

Now, we consider the multi-rogue waves in $(3+1)$-d NEE by taking $N > 1, n_i = 1\,(1 \le i \le N)$ and real values of $(p_1, \ldots p_N)$ in rational solutions (5). These rogue waves describes the superimposition between N individual fundamental line rogue waves in (z, y) plane. When $t \to \pm\infty$, the corresponding solution immerses in the constant background. However, N line waves approach the constant background and interact with each other in the intermediate times. What's more, the interaction can create complicated and interesting wave patterns. Finally, the N line wave go back to the constant background again.

To demonstrate this subclass of nonfundamental rogue waves more clearly. We take the $N = 2$ case into the first consideration. Letting $N = 2, n_1 = 1, n_2 = 1$ in Theorem 1, we can obtain the following explicit form of the second-order rogue

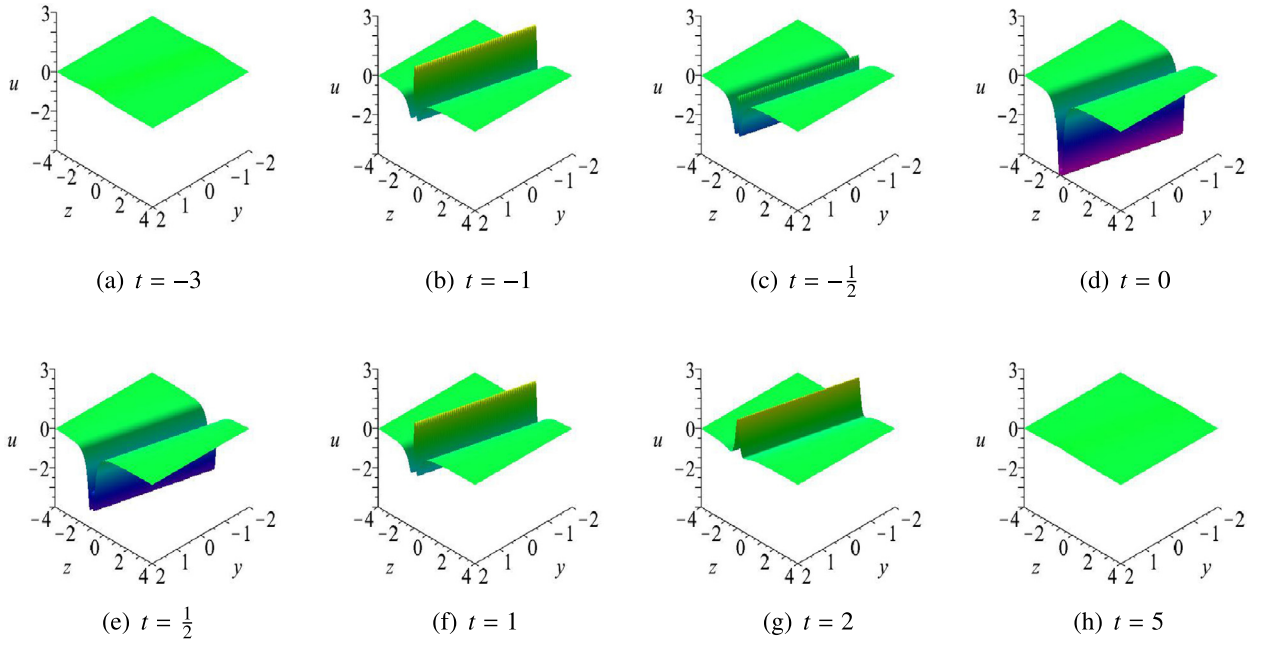

Fig. 3. (Color online) Dynamics of a fundamental rogue wave w (19) in $(3+1)$-NEE (1) with parameters $c_{11}=0, c_{10}=1, p_1=1, x=0$ in (y, z) panel. (For interpretation of the references to colour in this figure legend, the reader is referred to the web version of this article.)

wave solutions

$$w=-(2\log(\begin{vmatrix} m_{11} & m_{12} \\ m_{21} & m_{22} \end{vmatrix}))_{xx}, \tag{20}$$

where $m_{ij}=\frac{1}{p_i+p_j^*}[(\xi_i'-\frac{p_i}{p_i+p_j^*}+c_{i1})(\xi_j'^*-\frac{p_j^*}{p_i+p_j^*}+c_{j1}^*)+\frac{p_ip_j^*}{(p_i+p_j^*)^2}],\xi_i'$ is defined by Eq. (8), p_1, p_2 are free real parameters, and c_{11}, c_{21} are free complex parameters. The solution for parameters

$$p_1=1, p_2=\frac{3}{2}, c_{11}=0, c_{21}=0 \tag{21}$$

is shown in Figs. 4 and 5, which demonstrate the dynamics of multi-rogue waves in (y, z) plane and (x, t) plane respectively. As shown in Fig. 4, when $t\to-\infty$, there are no wave amplitudes exist in the constant background (see $t=-4$ panel). But when $t\to 0$, there are some complicated wave pattern approach from the constant background, and then they interact with each other (see $t=-2$ panel). What's more, the transient wave patterns become more intricate comparing to the fundamental rogue waves. At first, they behave as bright multi-rogue waves (see $t=-\frac{1}{3}, t=0$ panel), but alter very quickly, and turn into dark multi-rogue waves (see $t=-2, -1, -\frac{1}{2}$ panel). Whatever, they become the bright multi-rogue waves finally (see $t=1$ panel). When $t\to+\infty$, the line waves go back to the constant again.

The Fig. 5 demonstrates the dynamics of a two-rogue-wave solution (20) in (x, t) plane. It is seen that two line rogue waves arise from the constant background, and interact with each other (see the $y=\pm1$ panel). What's more, the region of their intersection reaches much higher amplitude (see the $y=o$ panel). Then line waves go back to the constant background and the interaction fades finally (see the $y=\pm\infty$ panel).

For larger N, these line rogue waves have qualitatively similar behaviors, except that more fundamental line rogue waves will arise and interact with each other, and more complicated wave fronts will form in the interaction region. For example, with $N=3$ and parameter choice

$$c_{11}=0, c_{21}=0, c_{31}=0, p_1=\frac{1}{2}, p_2=1, p_3=2, \tag{22}$$

the corresponding solution is shown in Figs. 6 and 7. As shown, the transient solution patterns become more intricate and its dynamics in (y, z) plane and (x, t) plane are shown clearly in Figs. 6 and 7. It is easy to find that this $(3+1)$-dimensional rogue waves keep decaying line profile in (y, z) plane and (x, t) plane.

3.3. High-order rogue waves in $(3+1)$-d NEE

Another subclass of nonfundamental rogue waves is the higher-order rogue waves, which can be obtained by taking $N=1$ and $n_i\geq 1$ in the rational solution (5) with a real value of p_1. For example, by setting $n_i=2$, the second-order rogue

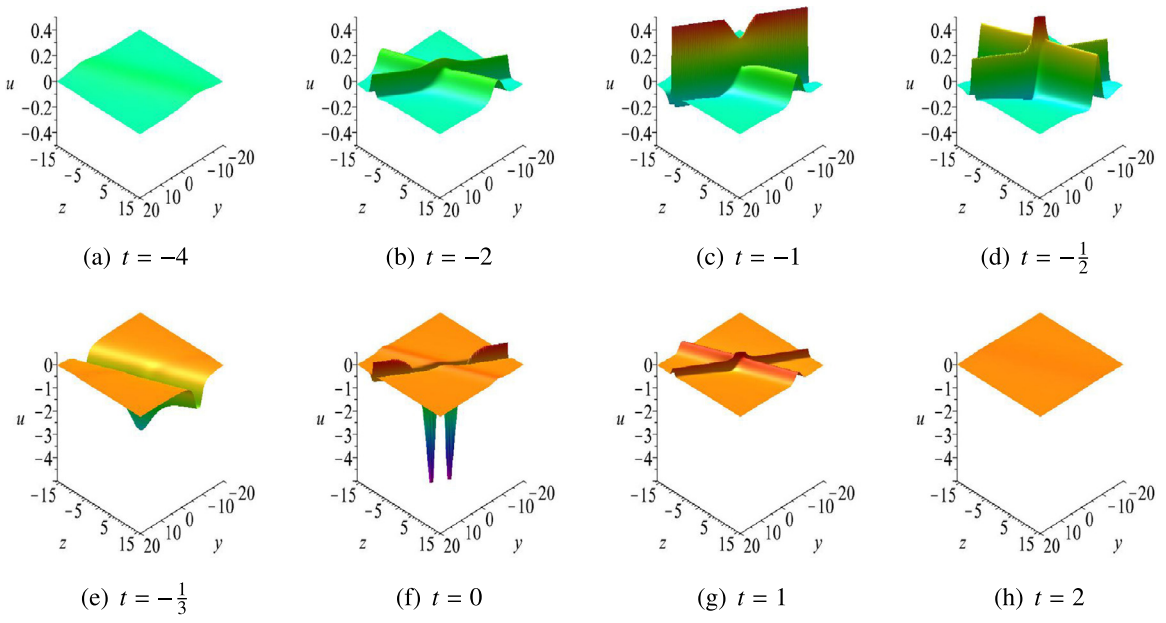

Fig. 4. (Color online) Dynamics of a two-rogue-wave solution (20) of $(3+1)$-NEE (1) in (y, z) plane for parameters (21) and $x = 0$. (For interpretation of the references to colour in this figure legend, the reader is referred to the web version of this article.)

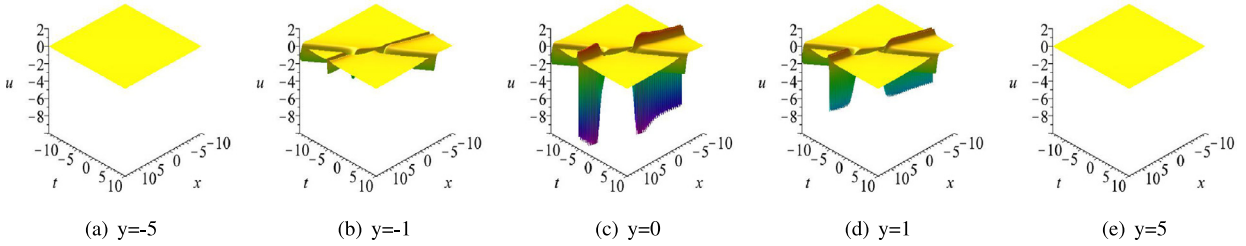

Fig. 5. (Color online) Dynamics of a two-rogue-wave solution (20) of $(3+1)$-NEE (1) in (x, t) plane for parameters (21) and $z = 0$. (For interpretation of the references to colour in this figure legend, the reader is referred to the web version of this article.)

waves can be obtained from Eq. (6) as

$$f = [(p_1\partial_{p_1} + \xi_1^{'})^2 + c_{12}][(p_1^*\partial_{p_1^*} + \xi_1^{'*})^2 + c_{12}^*]\frac{1}{p_1 + p_1^*}, \tag{23}$$

where $\xi_1^{'}$ is defined in Theorem 1, p_1 is a free real parameters,and c_{12} is a free complex parameters. As c_{11} can be treat as a shift of (x, y, t, z) axes, here we have set $c_{11} = 0$ in Eq. (5). What's more, the higher-order rogue waves with $n_i > 2$ can be obtained by a similar way.

Comparing to the multi-rogue waves demonstrated above, this second-order rogue waves possess different and funny profiles in Fig. 8. Firstly, these high-order rogue waves do not behave as line profiles in (y, z) plane. When $t \to \pm\infty$, the solutions do not uniformly approach the constant background, but a wave pattern with two downward peaks moving on the constant background (see $t = -5$ panel and $t = 4$ panel). When $t \to 0$, the state of the wave pattern changes frequently. At first, the maximum amplitude is downward (see $t = -3$ panel), but it changes to be upward in a short time (see $t = -1\,, 0$ panels), and finally it turns to upward again (see $t = 1$ panel). This kind of rogue waves in $(3+1)$-d NEE (1) is a distinctive phenomenon, as to the author's best knowledge, have also never been shown before.

Another different phenomenon is that, unlike the multi-rogue waves in (x, t) plane shown above, those higher-order rogue wave do not uniformly approach the constant background in (x, t) plane as $y \to \pm\infty$. Taking the second-order rogue waves with Eq. (23) as an example, which is shown in Fig. 9. It is seen that this solution also behaves as decaying line waves. However, just parts of their wave structures approach the constant background while the other parts moving on the constant background as $y \to \pm\infty$.

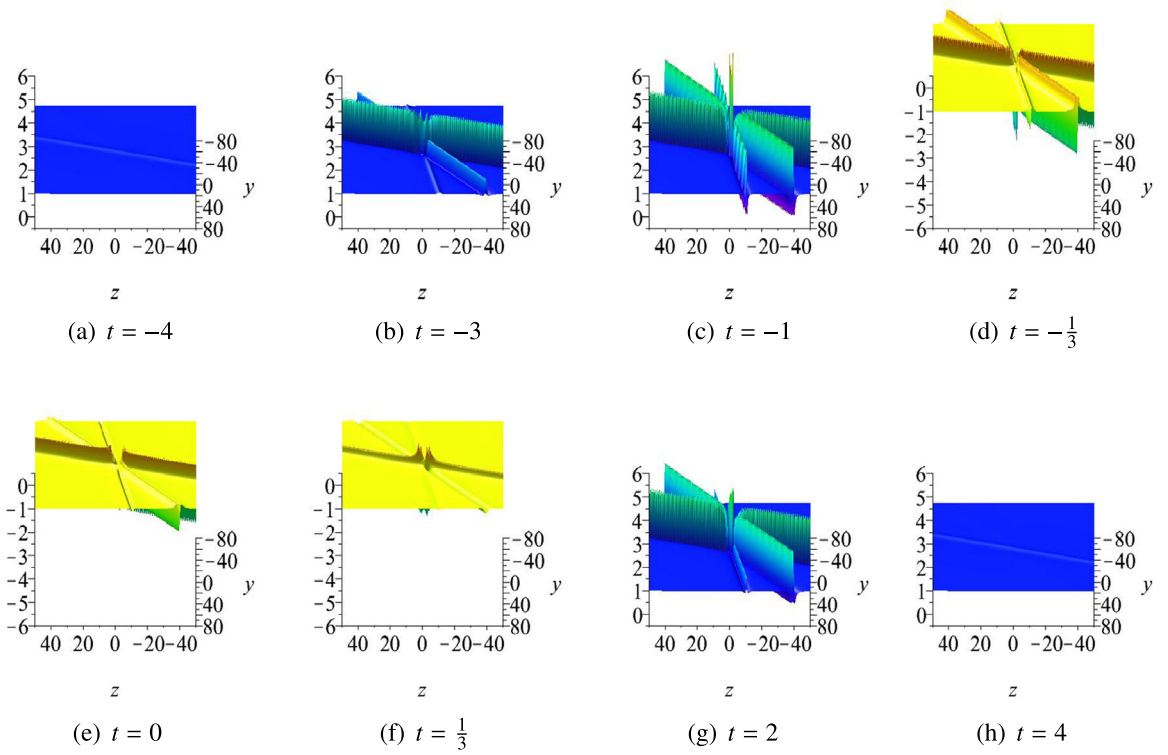

Fig. 6. (Color online) Dynamics of a three-rogue-wave solution of $(3+1)$-NEE (1) in (y, z) plane for parameters (22) and $x = 0$. (For interpretation of the references to colour in this figure legend, the reader is referred to the web version of this article.)

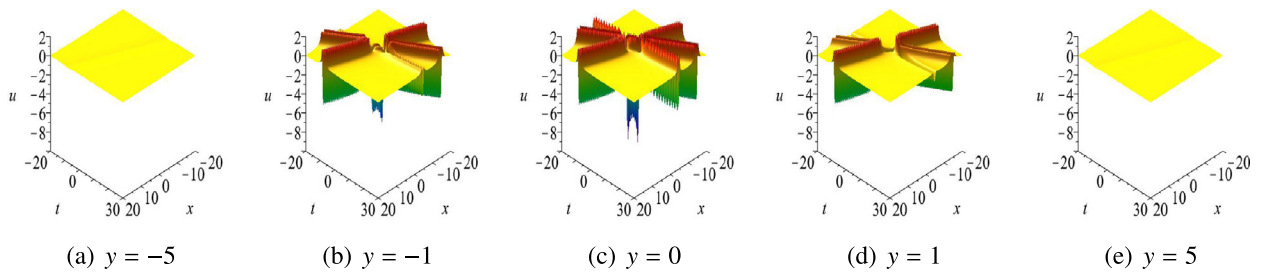

Fig. 7. (Color online) Dynamics of a three-rogue-wave solution of $(3+1)$-NEE (1) in (x, t) plane for parameters (22) and $z = 0$. (For interpretation of the references to colour in this figure legend, the reader is referred to the web version of this article.)

4. Summary and discussion

In summary, the general high-order rogue waves in $(3+1)$-d NEE (1) have been obtained by the bilinear method and KP reduction method, and the solutions are given in terms of determinants. As shown, the fundamental rogue waves (i.e., first-order rogue waves) are line localized waves which arise from the constant background with a line profile and then disappear into the constant background again. Two subclass of nonfundamental rogue wave (i.e., multi-rogue wave and high-order rogue wave) have been discussed in details. Multirogue waves describe the superposition of several fundamental rogue waves, and interesting curvy wave patterns would appear in the intermediate times. High-order rogue waves also possess decaying line profiles, which starts from a permanent lump and retreats back to it, and they possess wave patterns as parabolas. Moreover, the features and asymptotic behavior of rogue waves in $3+1$-d NEE (1) have been analyzed in details, and typical dynamics have been demonstrated in different plane(mainly in (x, t) plane and (y, z) plane) by three dimensional figures.

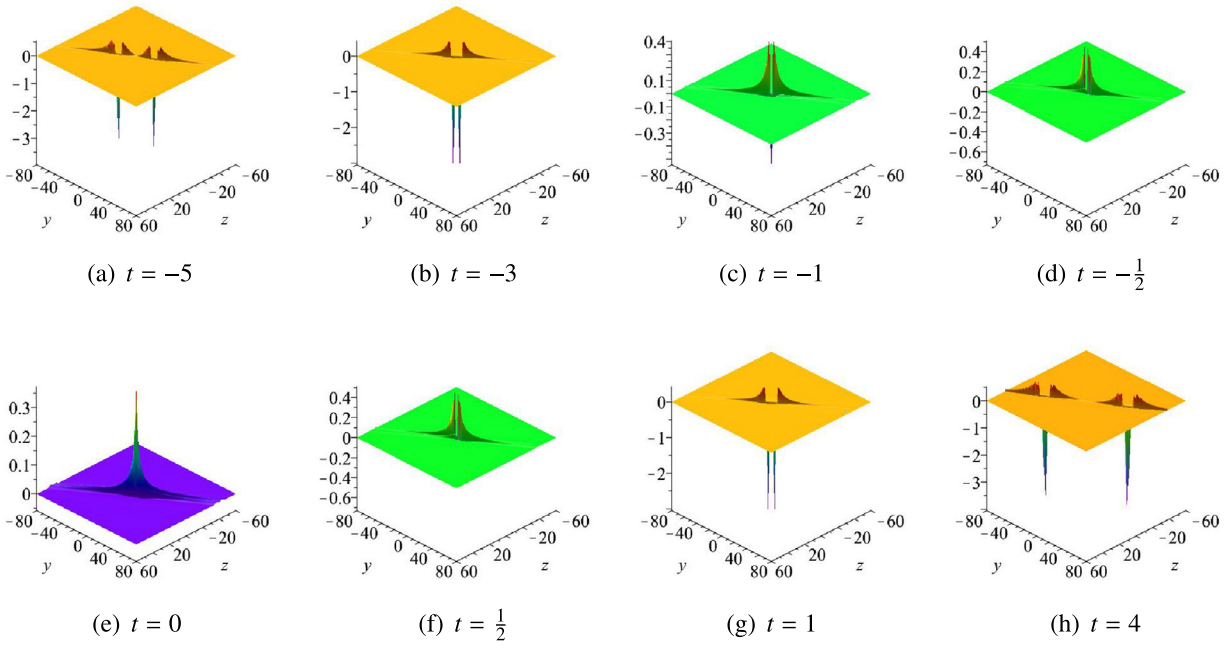

Fig. 8. (Color online) Dynamics of a two-rogue-wave solution (23) of $(3+1)$-NEE (1) in (y, z) plane with parameters $p_1 = 1, c_{11} = 0, c_{12} = 0, x = 0$. (For interpretation of the references to colour in this figure legend, the reader is referred to the web version of this article.)

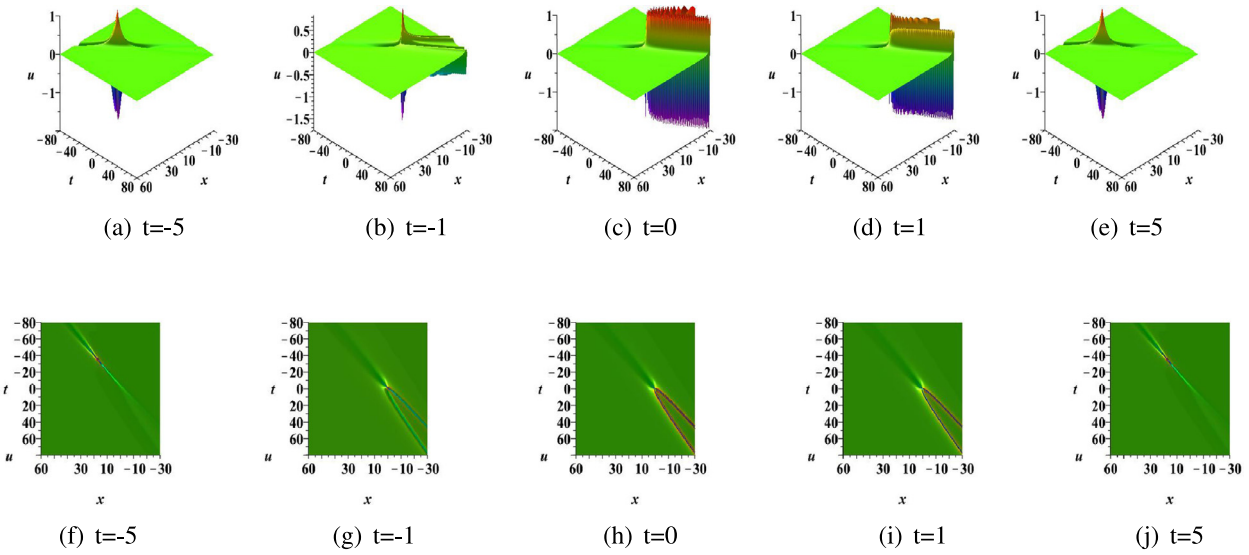

Fig. 9. (Color online) Dynamics of a two-rogue-wave solution (23) of $(3+1)$-NEE (1) in (x, t) plane with parameters $p_1 = 1, c_{11} = 0, c_{12} = 0, z = 0$. (For interpretation of the references to colour in this figure legend, the reader is referred to the web version of this article.)

Acknowledgment

The authors would like to express their sincere thanks to the referees for their enthusiastic guidance and help.

References

[1] Akhmediev N, Ankiewicz A, Taki M. Phys Lett A 2009;373:675.
[2] Bludov YV, Konotop VV, Akhmediev N. Phys Rev A 2009;80:033610.
[3] Bludov YV, Konotop VV, Akhmediev N. Eur Phys J Spec Top 2010;185:169.
[4] Montina A, Bortolozzo U, Residori S, Arecchi FT. Phys Rev Lett 2009;103:173901.
[5] Solli DR, Ropers C, Koonath P, Jalali B. Nature(London) 2007;450:1054.
[6] Höhmann R, Kuhl U, Stöckmann HJ, Kaplan L, Heller EJ. Phys Rev Lett 2010;104:093901.

[7] Kharif C, Pelinovsky E, Slunyaev A. Rogue waves in the ocean. Berlin: Springer; 2009.
[8] Ganshin AN, Efimov VB, Kolmakov GV, Mezhov-Deglin LP, McClintock PVE. Phys RevLett 2008;101:065303.
[9] Moslem WM. Phys Plasmas 2011;18:032301.
[10] Bailung H, Sharma SK, Nakamura Y. Phys Rev Lett 2011;107:255005.
[11] Yan ZY. Commun Theor Phys 2010;54:947.
[12] Peregrine DH. J Aust Math Soc B 1983;25:16.
[13] Dubard P, Matveev VB. Nat Hazards Earth Syst Sci 2011;11:667.
[14] Akhmediev N, Ankiewicz A, Soto-Crespo JM. Phys Rev E 2009;80:026601.
[15] Dubard P, Gaillard P, Klein C, Matveev VB. Eur Phys J Spec Top 2010;185:247.
[16] Ankiewicz A, Kedziora DJ, Akhmediev N. Phys Lett A 2011;375:2782.
[17] Guo B, Ling L, Liu QP. Phys Rev E 2012;85:026607.
[18] Kedziora DJ, Ankiewicz A, Akhmediev N. Phys Rev E 2011;84:056611.
[19] Ohta Y, Yang JK. Proc R Soc A 2012;468:1716.
[20] He JS, Zhang HR, Wang LH, Porsezian K, Fokas AS. Phys Rev E 2013;87:052914.
[21] Wang LH, Porsezian K, He JS. Phys Rev E 2013;87:053202.
[22] Wang X, Li YQ, Huang F, Chen Y. Commun Nonlinear Sci Numer Simulat 2015;20:434.
[23] Wang X, Cao JI, Chen Y. Phys Scr 2015;90:105201.
[24] Qiu DQ, He JS, Zhang YS, Porsezian K. Proc R Soc A 2015;471:20150236.
[25] Liu W, Qiu DQ, He JS. Commun Theor Phys 2015;63:525.
[26] He JS, Xu SW, Porsezian K. Phys Rev E 2012;86:066603.
[27] He JS, Zhang HR, Wang LH, Porsezian K, Fokas AS. Phys Rev E 2013;87:052914.
[28] Rao JG, Wang LH, Zhang Y, He JS. Commun Theor Phy 2015;64:605.
[29] Onorato M, Residori S, Bortolozzo U, Montinad A, Arecchi FT. Phys Reports 2013;528:47.
[30] Ohta Y, Yang JK. Phys Rev E 2012;86:036604.
[31] Ohta Y, Yang JK. J Phys A: Math Theor 2013;46:105202.
[32] Dudley JM, Dias F, Erkintalo M, Genty G. Nature Photonics 2014;8:755.
[33] Dubard P, Matveev VB. Nonlinearity 2013;26:93.
[34] Chen JC, Chen Y, Feng BF. Phys Lett A 2015;379:1510.
[35] Mu G, Qin ZY. Nonlinear Anal Real World Appl 2014;18:1.
[36] Zhang Y, Sun YB, Xiang W. Appl Math Comput 2015;263:204.
[37] Zha QL. Phys Lett A 2013;377:3021.
[38] Geng XG. J Phys A, Math Gen 2003;36:2289.
[39] Wazwaz AM. ApplMathComput 2009;215:1548.
[40] Geng XG, Ma YL. PhysLettA 2007;369:285.
[41] Zha QL, Li ZB. Mod Phys Lett B 2009;23:2971.
[42] Zha QL, Li ZB. Mod Phys Lett B 2008;22:2945.
[43] Hirota R. The direct method in soliton theory. Cambridge,UK: Cambridge University Press; 2004.
[44] Jimbo M, Miwapubl T. RIMS, Kyoto Univ 1983;19:943.